Design of real-time confocal microscopy using spectral encoding technique and slit aperture

Jeongmin Kim*[a], DongKyun Kang[a], DaeGab Gweon[a],
YeongSoo Sohn[b] and Hyungsuck Cho[c]

[a]Nano Opto Mechatronics (NOM) Laboratory, Mechanical Eng. Dept., Korea Advanced Institute of Science and Technology (KAIST), Guseong-dong, Yuseong-gu, Daejeon, Korea, 305-701
[b]Dukin Co., Ltd, Hwaam-dong, Yuseong-gu, Daejeon, Korea, 305-348
[c]Optomechatronic Systems and Machine Intelligence Laboratory, Mechanical Eng. Dept., KAIST, Guseong-dong, Yuseong-gu, Daejeon, Korea, 305-701

ABSTRACT

New confocal microscopy having no mechanical beam scanning devices is proposed. The proposed system can get two-dimensional information of a specimen in real-time by using spectral encoding technique and slit aperture. Spectral encoding technique is used to encode one-dimensional lateral information of the specimen in wavelength by a diffraction grating and a broadband light source. The modeling of the optical system is conducted. The effect of slit width variation on the axial response of the system is evaluated by numerical simulation based on the wave optics. Proper width of the slit aperture which plays a crucial role of the out-of-focus blur rejection is determined by a compromise between axial resolution and signal intensity from the simulation result. Design variables and governing equations of the system are derived on the assumption of a lateral sampling resolution of 50 nm. The system is designed to have a mapping error less than the half pixel size, to be diffraction-limited and to have the maximum illumination efficiency. The designed system has a FOV of 12.8 um × 9.6 um, a theoretical axial FWHM of 1.1 um and a lateral magnification of -367.8.

Keywords: Confocal microscopy, spectral encoding, slit aperture, real-time

1. INTRODUCTION

Confocal microscopy has been getting popular in various fields thanks to its unique optical sectioning property with the enhanced optical resolution over conventional widefield optical microscopy by eliminating out-of-focus light. In cell biology, confocal microscopy is used to get three-dimensional information about membrane potentials, intracellular free calcium activities as well as structures in living cells.[1] There has been an increase in the use of confocal microscopy for biomedical applications such as the detection of tissue abnormalities for the early stage identification of diseases like skin cancers, *in vivo* measurement of the human cornea and the intact inner ear and so on.[1,2] Surface characteristics of wafers and LCDs in semiconductor industry and critical dimensions of products in nano/micro manufacturing have also being inspected by real-time confocal microscopy for mass production.[1] The real-time imaging capability of confocal microscopy is essential for all of the fields mentioned above.

Almost commercial real-time confocal microscopes use beam scanning devices or rotating Nipkow disks. Acoustic optic deflectors (AODs), polygon mirrors, galvano mirrors are typical beam scanning devices[3] used to deflect the beam incident on the back aperture of the objective lens so that they can move the position of the focal spot within the specimen. However, they increase system complexity, and control electronics of them are mostly expensive.[4] Vibrations caused by them result in decrease of a signal-to-noise ratio (SNR) and an image distortion.[4] Moreover, inherent loads by serial data collection limit the rates of image acquisition and subsequent processing. On the other hand, confocal microscopes having rotating Nipkow disks, spiral array of the pinholes, have a problem of image degradation induced by optical cross talk among pinholes. They also suffer from low illumination efficiencies which restrict the use of the Nipkow disks to the real-time applications.[4] It has been shown that spectral encoding is one of promising techniques

* minism@kaist.ac.kr; phone 82 42 869 5225; fax 82 42 869 5225; http://nom.kaist.ac.kr

Optomechatronic Sensors and Instrumentation, edited by Yasuhiro Takaya, Proc. of SPIE Vol. 6049, 604906, (2005)
0277-786X/05/$15 · doi: 10.1117/12.647953

which eliminate the need of a fast scanning device in confocal microscopy[5,6] and suitable for real-time frame rates (more than 30 frames/s).

The object of this study is to propose and design a new type of real-time confocal microscopy with no mechanical scanning units. The principle of operation for the proposed system is explained. Simulation of the axial response of the proposed system has been carried out, and the system is designed.

2. CONFIGURATION

2.1 Principle of operation

Figure 1 shows the configuration of the proposed confocal microscopy. A broadband line source is imaged on a plane at which a slit places by a magnification factor determined by the ratio of an effective focal length of a collector to that of a condenser. Light emanating from the slit aperture is dispersed by a transmission diffraction grating, and a series of the slit image of different wavelengths is illuminated on the specimen plane in two-dimensions. The remitted light from the specimen is encoded by the same grating. The confocal effect, the physical rejection of out-of-focus information of the specimen, at the slit occurs mainly in the direction of the slit width as the encoded light signal passes through it. Therefore, the proposed system can have the enhanced optical resolution and the depth discrimination property compared to conventional widefield optical microscopy. The confocal signal from the slit is then decoded by another transmission diffraction grating. Finally, a CCD camera detects the two-dimensional confocal signal at a time and converts it into an equivalent electronic signal for display at a PC.

The proposed system does not require scanning units by using the spectral encoding technique and the slit aperture, so the rates of image acquisition are not limited by the scanning speed of them. A direct view capability of the system can make the rates of image acquisition very fast even up to tens of thousands of frames per second. The system is free of image degradation from vibrations of scanning units and can be miniaturized at a low cost.

2.2 System configuration

The proposed system can be classified as illumination optics, confocal optics and imaging optics.

Illumination optics provides a polarized and filtered broadband line source for confocal optics. The broadband line source made from a halogen lamp and a line light guide is placed at the front focal length of the collector for illumination

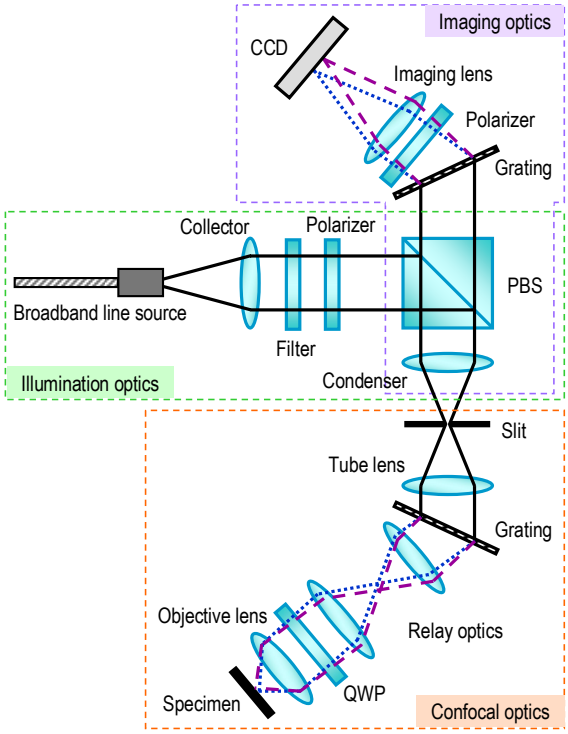

Figure 1 Configuration of the proposed confocal microscopy

optics to be the infinity-corrected optics. A filter is used to restrict the transmission of the wavelength band not concerned. A polarizer and a polarized beam splitter (PBS) prevent stray lights reflected directly at the slit surface from being detected at the CCD image sensor. The S-polarized light is incident upon confocal optics.

Two-dimensional illumination of the specimen and the acquisition of the confocal signal have been done in confocal optics. A quarter-wave plate (QWP), relay optics and a grating are interposed between a tube lens and an objective lens in confocal optics. The QWP enables the remitted light from the specimen to be P-polarized so that the confocal signal can proceed to imaging optics. Relay optics is essential for the back focal plane of the objective lens to be conjugate with a plane where the grating is. By doing so, the numerical aperture (NA) of the objective lens can be fully used, and uniformity of illumination intensity with wavelength is improved with less light loss at the back aperture of the objective lens. The grating disperses the S-polarized light coming from illumination optics and encodes the remitted one-dimensional specimen information in wavelength. The confocal signal is P-polarized.

The confocal signal is decoded by a grating in imaging optics and is detected at the CCD image sensor. A polarizer is used to remove stray lights except the P-polarized confocal signal. The distance between an imaging lens and the CCD image sensor is equal to the back focal length of the imaging lens.

3. ANALYSIS

Since confocal optics dominantly affected the overall performance of the proposed system, variations in its axial response with slit width needed to be evaluated.

3.1 Modeling of confocal optics

By neglecting the polarizing property of light and considering only a center wavelength λ_{CWL} of the system, confocal optics could be reduced to an equivalent thin lens as shown in Figure 2. A lateral magnification of the model, M, was determined by the objective lens focal length f_{OL}, relay optics angular magnification M_{RO} from the slit to the specimen and the tube lens focal length f_{tube}. Coordinates of the illuminating slit, the specimen and the confocal slit were assigned like Figure 3. Lens L1 for illuminating the specimen and L2 for collecting the remitted light were placed on the ξ_1-η_1 lens plane and the ξ_2-η_2 lens plane respectively.

$$(v_x, v_y) = \frac{2\pi}{\lambda}(x_1, y_1)\frac{a}{f_{OL}} \approx \frac{2\pi}{\lambda} NA(x_1, y_1)$$
$$u = \frac{2\pi}{\lambda} z_1 \frac{a^2}{f_{OL}^2} \approx \frac{2\pi}{\lambda} NA^2 z_1 \qquad (1)$$

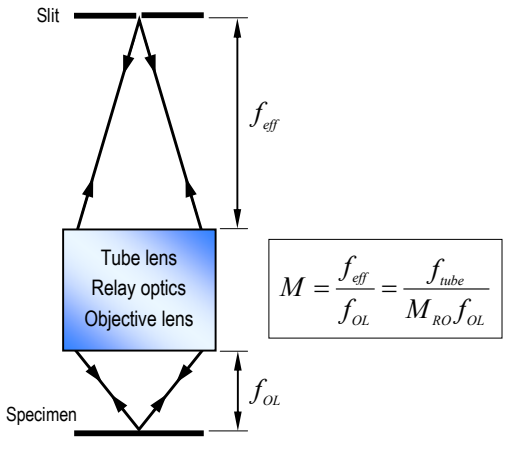

Figure 2 Simplified thin lens model of confocal optics

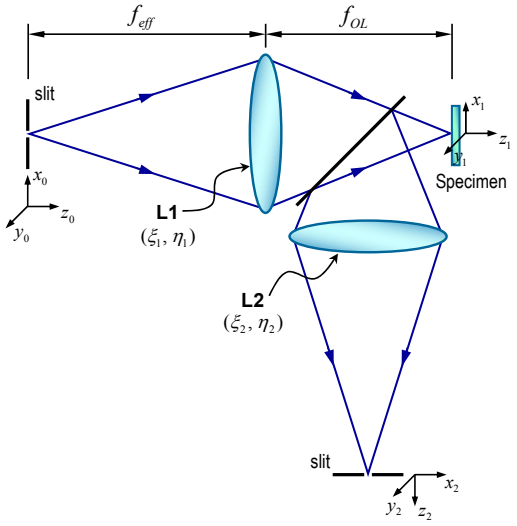

Figure 3 Schematic diagram of confocal optics

3.2 Intensity Point Spread Function (IPSF)

To derive the IPSFs of L1 and L2, we used optical coordinates[7], (1), of the specimen space as a reference to normalize the effect of the wavelength, the tube lens, relay optics and the objective lens. The IPSF of L1 was derived from the Fresnel diffraction formula[8] in the form of

$$IPSF_{L1} = \left|h_{L1}^{'}(v_x, v_y, u)\right|^2 = \left|\int_{-\infty}^{\infty}\int_{-\infty}^{\infty} P(\xi_1^{'}, \eta_1^{'})\, \mathrm{e}^{-\frac{i}{2}u\left(\xi_1^{'2}+\eta_1^{'2}\right)}\, \mathrm{e}^{i\left(\xi_1^{'}v_x+\eta_1^{'}v_y\right)}\, d\xi_1^{'} d\eta_1^{'}\right|^2 \tag{2}$$

where $P(\xi_1^{'}, \eta_1^{'})$ is the normalized pupil function of L1. The IPSF of L2 resulted in the same form as that of L1 in the optical coordinates because it was rotationally symmetric and confocal opics was the reflection type.

3.3 Simulation of the axial response

For a plane mirror having a reflectance of one in the specimen space, the intensity distribution of the remitted light at the confocal slit was calculated as

$$I_{slit}(v_x, v_y, u) = S(v_x, v_y) \otimes_3 IPSF_{L1} \otimes_3 IPSF_{L2} \tag{3}$$

where $\otimes_3$ denoted the convolution operation and $S(v_x, v_y)$ denoted the intensity sensitivity, which represented the slit geometry with the intensity distribution of the incoherent light within the aperture. Normalized slit width v_w, related to the physical slit width as

$$w = M\frac{\lambda_{CWL}}{2\pi\, NA} v_w \tag{4}$$

, was used in simulation. The axial response (5) was obtained as a function of the defocus distance u of the plane mirror by integrating intensity values of the remitted light which passed through the slit aperture. (Figure 4)

$$I_{signal}(u) = \int_{-\frac{v_L}{2}}^{\frac{v_L}{2}}\int_{-\frac{v_w}{2}}^{\frac{v_w}{2}} I_{slit}(v_x, v_y, u)\, dv_x dv_y \tag{5}$$

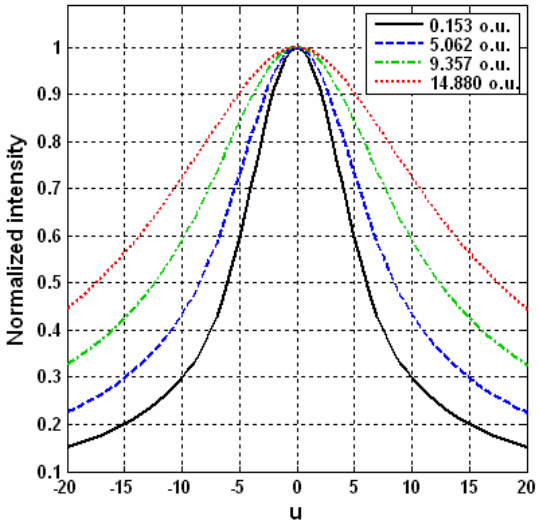

Figure 4 Simulation result of normalized axial responses with the normalized slit width in the optical coordinates

3.4 Axial resolution and signal intensity

From the simulation result of the axial response, variations in the maximum signal intensity (when $u = 0$) and the axial resolution, which was inversely proportional to the FWHM, with the normalized slit width were calculated as shown in Figure 5. The normalized slit width of 2.61 optical unit (o.u.) based on a compromise between axial resolution and signal intensity was chosen as the design value. The FWHM of confocal optics at the design value was 15.507 o.u. and the physical silt width was related to (6).

$$w = 0.415 \frac{\lambda_{CWL}}{NA} \frac{f_{tube}}{f_{OL} M_{RO}} \tag{6}$$

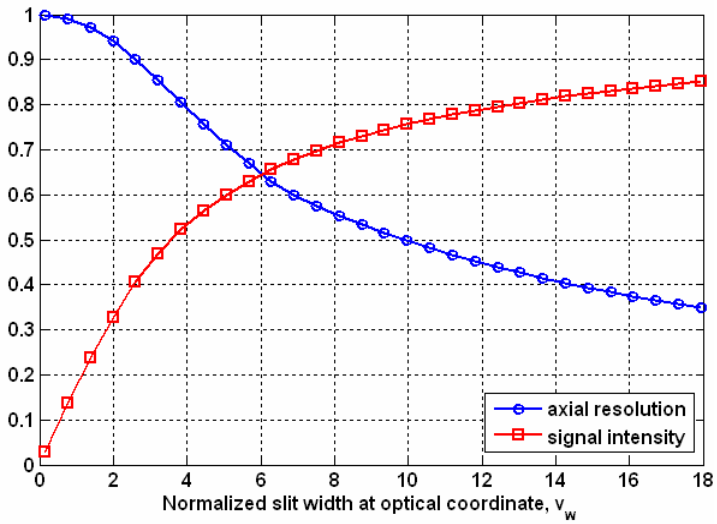

Figure 5 Variations in the normalized axial resolution and signal intensity of confocal optics with the normalized slit width from the simulation result

4. DESIGN

4.1 Confocal optics and imaging optics

A lateral sampling resolution of 50 nm was selected as one of design goals. Then, from the Nyquist sampling criterion,

Table 1 Design variables of confocal optics and imaging optics

Design variable	Notation
Slit width	w
Slit length	L
Tube lens focal length	f_{tube}
Full field angle caused by L and the tube lens	$\theta_{full\_field\_L}$
Wavelength bandwidth	$\Delta\lambda$
Grating groove density	G
Grating diffraction angle at λ_{CWL}	θ_d
Grating dispersion angle	$\theta_{full\_field\_Grating}$
Relay optics angular magnification	M_{RO}
Imaging lens focal length	$f_{imaging}$

the required lateral magnification of the system from the specimen to the CCD was -370 to sample a 20 nm × 20 nm area of the specimen by a CCD pixel of 7.4 um × 7.4 um. The objective lens used had 0.95 NA and the 1.8 mm focal length. The center wavelength of 405 nm was chosen. The physical sensing area of the 30 Hz progressive scan CCD camera was 4.736 mm × 3.552 mm (640 pixels × 480 pixels). Assuming that two gratings of the system were identical and the focal length of the tube lens was equal to that of the condenser, design variables of confocal optics and imaging optics were given in Table 1. Governing equations to meet the lateral magnification of -370 were derived as follows.

• Grating dispersion angle required: $$\theta_{full\_field\_Grating} = \frac{\theta_{full\_field\_OL}}{M_{RO}} \quad (7)$$

• Field of view (FOV) matching: $$\theta_{full\_field\_L} = \frac{3}{4}\theta_{full\_field\_Grating} \quad (8)$$

• Full field angle caused by L and the tube lens: $$\theta_{full\_field\_L} = \frac{L}{f_{tube}} \quad (9)$$

• Diffraction angle at the center wavelength: $$\theta_d = \sin^{-1}\left(\frac{G\lambda_{CWL}}{2}\right) \quad (10)$$

• Grating dispersion angle generated: $$\theta_{full\_field\_Grating} = \frac{G}{\cos\theta_d}\Delta\lambda \quad (11)$$

• The imaging lens focal length required: $$f_{imaging} = \frac{4.736}{\theta_{full\_field\_Grating}} \quad (12)$$

Ten design variables and seven governing equations, including (6), were obtained. Derivation of (10) and (11) based on the diffraction grating equation.[9] There were many cases satisfying the lateral magnification condition because the number of variables were three more than that of equations. However, the slit width w, the grating groove density G and the relay optics angular magnification M_{RO} were the variables whose values were restricted to some of specific ones in commercial products. We found the aspect ratio of the slit aperture kept constant value 54.26, from (7), (8), (9) and (12), irrespective of design variables, so a commercial slit of 50 um width and 3 mm length was picked up. The groove density of the diffraction gratings was chosen as 2400 lines/mm. Simple calculation showed M_{RO} affected variations in the lateral magnification of the system which was undesirable and which should be limited within the FOV

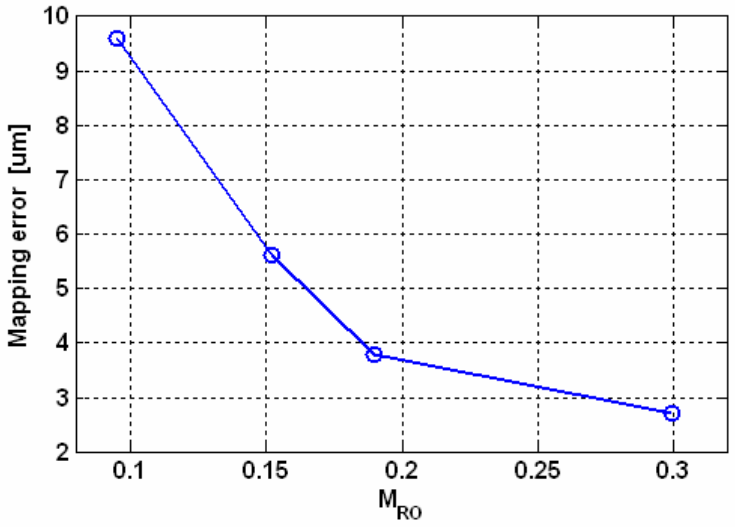

Figure 6 Simulation result of the effect of relay optics angular magnification on the mapping error

(12.8 um×9.6 um). Therefore, the actual image position in the CCD of a point object within FOV was different from the image position when assumed to maintain constant lateral magnification regardless of the point object position. For quantitative analysis of that, the mapping error was defined as the maximum of those position errors in the CCD plane caused by variations in the lateral magnification of the system within the FOV. We simulated the mapping error for various M_{RO} values by using the ZEMAX software. Distances between optical components were optimized to have the minimum root mean square (RMS) wavefront errors.

From another design goal of the mapping error less than the half pixel size, the design value of M_{RO} was 0.19. (Figure 6) The other of the design goals was diffraction-limited performance, and it was satisfied at M_{RO} of 0.19 as shown in Figure 7. Designed values of confocal optics and imaging optics were in Table 2.

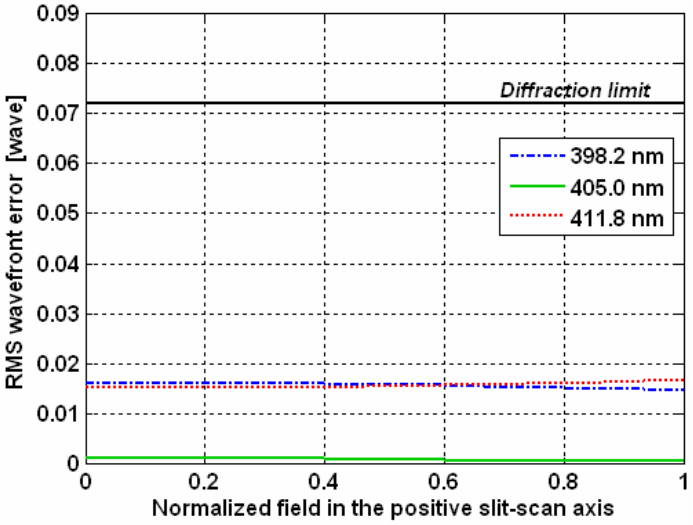

Figure 7 Simulation result of the RMS wavefront error satisfying diffraction-limited performance

Table 2 Design results of confocal optics and imaging optics

Design variable	Designed value
w	50 um
L	2.713 mm
f_{tube}	100 mm
$\theta_{full\_field\_L}$	1.607°
$\Delta\lambda$	13.62 nm
G	2400 lines/mm
θ_d	29.1°
$\theta_{full\_field\_Grating}$	2.143°
M_{RO}	0.19 (= 19 mm/100 mm)
$f_{imaging}$	125 mm

4.2 Illumination optics

The 200 um×20 mm, ±20° broadband line source was used to supply light to the 50 um×2.713 mm slit aperture. The designed focal length of the condenser was 100 mm. The only variable we could make a change in illumination optics was the collector focal length in the range of 50 mm to 400 mm. When the collector focal length was 50 mm, dominant light loss occurred at the slit because the slit prevented much of light from passing through it. On the other hand, vignetting at the collector was the main reason of light loss when the collector focal length was 400 mm.

Design goal of illumination optics was to maximize the illumination efficiency defined as (13) based on the ray tracing. The term "rays detected" here meant the number of rays passed through the slit aperture. The maximum illumination efficiency of 0.7 % was obtained at the collector focal length of 150 mm. The designed distances between optical components consisting of the proposed system were shown in Figure 9.

$$Illumination\ \ efficiency = \frac{rays\ detected}{all\ rays\ launched} \times 100 \tag{13}$$

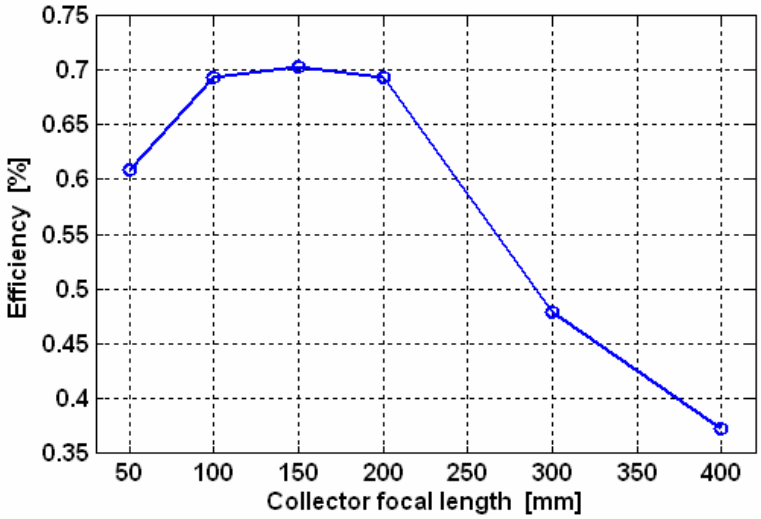

Figure 8 The maximum illumination efficiency of 0.7 % at 150 mm collector focal length (simulation result)

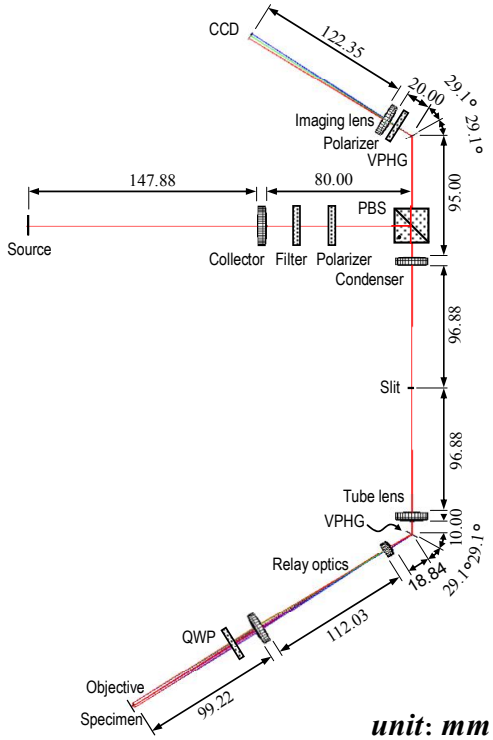

Figure 9 Designed geometry of the proposed system

5. CONCLUSIONS

The use of spectral encoding technique and slit aperture in confocal microscopy seems to be an excellent method for easy and cheap realization of real-time imaging. The frame rate of such a system is only limited by signal intensity or output frequency of the CCD camera, not by scanning units. Slit width and mapping error are critical factors affecting the performance of the system and should be considered in design. In this study, we set the design points where the slit width makes 10% decrease in the normalized axial resolution and the mapping error is less than the half pixel size. It is expected that the proposed system can also contribute to the miniaturization of confocal microscopy.

ACKNOWLEDGMENTS

This study was supported by Ministry of Commerce, Industry and Energy (MOCIE) of Korea and Korea Science and Engineering Foundation (KOSEF).

REFERENCES

1. T. Wilson and B. R. Masters, "Confocal microscopy", Appl. Opt., **33**, pp. 565-566, 1994
2. I. Krohne, T. Pfeifer, F. Bitte, M. Zacher, R. Meier, "New method for confocal microscopy and its endoscopic application", Novel Optical Instrumentation for Biological Applications, Albert-Claude Boccara, Proc. of SPIE-OSA Biomedical Optics, **5143**, pp. 281-288, 2003
3. R. H. Webb, "Optics for laser rasters", Appl. Opt., **23**, pp. 3680-3683, 1984
4. J. B. Pawley, *Handbook of biological confocal microscopy*, 2nd ed., pp. 459-462, Plenum, New York, 1995
5. G. J. Tearney, M. Shishkov, B. E. Bouma, "Spectrally encoded miniature endoscopy", Opt. Lett., **27**, pp. 412-414, 2002
6. G. J. Tearney, R. H. Webb, B. E. Bouma, "Spectrally encoded confocal microscopy", Opt. Lett., **23**, pp. 1152-1154, 1998
7. Min Gu, *Principles of Three-Dimensional Imaging in Confocal Microscopes*, pp. 20-35, World Scientific, Singapore, 1996
8. Min Gu, *Principles of Three-Dimensional Imaging in Confocal Microscopes*, pp. 15-19 , World Scientific, Singapore, 1996
9. J. W. Goodman, *Introduction to Fourier Optics*, 3rd ed., pp. 463-464, Roberts & Company, Colorado, 2005